ELSEVIER

Journal of Magnetism and Magnetic Materials 182 (1998) 81–88

Journal of magnetism and magnetic materials

3D micromagnetic model of finite linear defects in antiferromagnetically coupled multilayers

D.V. Berkov[a], N.L. Gorn[a], R. Mattheis[a,*], T. Zimmermann[b]

[a] *Institut für Physikalische Hochtechnologie e.V., PF 100 239, D-07702, Jena, Germany*
[b] *Siemens AG, Bereich HL, Wernerwerksstr., D-93009, Regensburg, Germany*

Received 27 January 1997; received in revised form 4 June 1997

Abstract

A 3D micromagnetic model for the study of the influence of finite linear structural defects on the remagnetization processes in antiferromagnetically coupled multilayers is presented (such defects are assumed to induce the local ferromagnetic coupling between adjacent magnetic layers). Some new features of 360°-domain walls predicted by the previous model where the defect was assumed to be infinitely long are observed. It is shown that the annihilation field of such walls strongly depends on the defect configuration, whereas the wall width is determined by the parameters of the undisturbed layer only. Consequences for the comparison of our results with experimental data are drawn.

Keywords: Micromagnetism; Multilayers; Linear defects; Antiferromagnetic coupling; Domain walls; Lorentz microscopy

1. Introduction

With this letter we continue our study of the influence of linear structural defects on the remagnetization processes in magnetic multilayers Co/Cu. Such multilayers demonstrate the giant magnetoresistance effect (GMR) at room temperature and hence are of a great interest for various applications (first of all for magnetic sensors). But irreversible magnetization processes leading to the hysteresis both in the magnetization curves and in the field dependence of the magnetoresistance [1–3] prevent the construction of reliable practical devices based on such multilayers.

The natural explanation of this irreversible behaviour is based on the concept of structural defects which could locally affect the interlayer coupling and even change its sign. Several models of such defects for a system of two coupled layers under quite strong additional assumptions were investigated in Refs. [3, 4]. In Ref. [5] we proposed a model, where linear structural defects arising during the growth process were suggested to be responsible for the irreversible remagnetization.

* Corresponding author. Tel.: + 49 36 41 657723; fax: + 49 36 41 657700; e-mail: mattheis@ipht-jena.de.

0304-8853/98/$19.00
PII S0304-8853(97)00219-9

Such defects manifest themselves, in particular, in changing the interlayer distances along the defect line which (as mentioned above) cannot only weaken the normal antiferromagnetic (AF) coupling between the layers but also result in the ferromagnetic (FM) coupling along the defect lines.

In Ref. [5] we studied the model where such a linear defect (inducing a FM coupling between adjacent magnetic layers) was assumed to be straight and infinitely long. In addition, magnetic moments during the remagnetization process were allowed to rotate only in the layer plane – the assumption which seemed to be justified by the large shape anisotropy of a single layer. But the most interesting result found in our simulations – the appearance of 360°-domain walls during the remagnetization process – could be merely artificial due to this in-plane restriction.

For this reason this purely 2D model was extended in such a way that magnetic moments were allowed to rotate in 3D (i.e., out of plane also) [6]. This lead to a substantial reduction of the annihilation field of 360°-domain walls when compared with Ref. [5], but the field region of their existence was still very wide [6] resulting in large tails on the hysteresis loops which were never observed experimentally. On the other hand, the effect of the finite defect length should be also taken into account. Both circumstances required further extension of the model trying to achieve more reasonable agreement with the experimental results.

2. Micromagnetic model

The main qualitative difference between our previous model [6] and real linear defects which are assumed to appear along the grain boundaries is that real defects obviously have a finite length. The presence of the end of the defect line could substantially influence as well the geometry of domain walls arising near such a defect as its annihilation field. For this reason we developed a full 3D model where a semi-infinite defect was embedded in a multilayer structure as shown in Fig. 1. As in Refs. [5, 6] we assumed that the interlayer coupling along the defect line is ferromagnetic in contrast

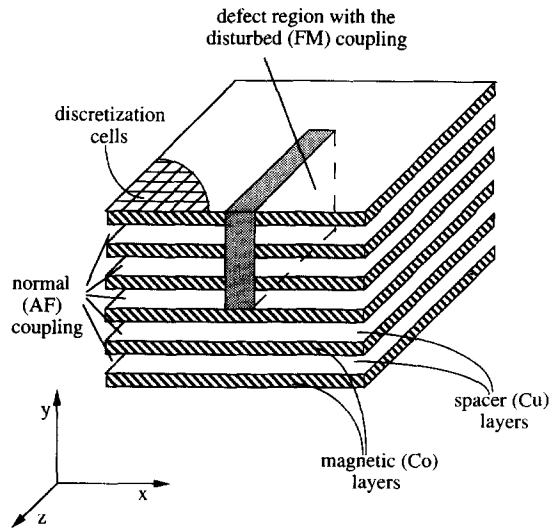

Fig. 1. Multilayer structure with the semi-infinite defect.

to the antiferromagnetic interlayer coupling in the defect-free regions.

We also assumed that magnetic layers are thin enough to neglect the magnetization variation perpendicular to the layer plane inside a single layer and hence discretized our system as shown in Fig. 1 – one cell layer in y-direction per magnetic layer. As it was explained in Refs. [5, 6] in the case of Co/Cu multilayers we can neglect the crystallographic anisotropy energy and take into account the demagnetizing energy simply as the shape anisotropy energy of a thin magnetic film. Altogether, for our 3D model we have to minimize the total system energy of the form (the construction of this expression proceeds exactly in the same way as in Ref. [6])

$$E_{\mathrm{tot}}/\Delta V = -M_s^2 \sum_i \boldsymbol{m}_i \boldsymbol{h}_{0i} - A\left(\frac{1}{\Delta x^2}\sum_{\langle i,j\rangle_x} \boldsymbol{m}_i\boldsymbol{m}_j + \frac{1}{\Delta z^2}\sum_{\langle i,j\rangle_z} \boldsymbol{m}_i\boldsymbol{m}_j\right) - \frac{1}{\Delta y}\sum_{\langle i,j\rangle_y} J_{ij}\boldsymbol{m}_i\boldsymbol{m}_j + 2\pi M_s^2 \sum_i m_{y,i}^2. \quad (1)$$

Here $\langle i,j\rangle_x$ means a summation over nearest neighbors in the x-direction (the same for y and z), M_s (=1400 G for Co) denotes the saturation magnetization of the material, $\boldsymbol{m}_i$ is the unit vector

pointing in the magnetization direction in the ith cell, the reduced external field is defined as $\boldsymbol{h}_0 = \boldsymbol{H}_0/M_s$, A ($=10^{-6}$ erg/cm^2 for Co) is the ferromagnetic exchange constant of the material, J_{ij} are interaction constants characterizing interlayer coupling between cells i and j which belong to adjacent layers. The geometry of the problem is defined by the sizes of the discretization cell in corresponding directions Δx, Δy, Δz and its volume ΔV.

Magnetic and structural parameters for the multilayer structure under study were chosen according to their values determined experimentally. In the defect-free region (for a perfect multilayer) we set $J_{ij} = J_{af}$ ($= -0.2$ erg/cm^2 for our system [6, 7]). In the region occupied by the defect the interlayer coupling was set to Refs. [8, 6] $J_{ij} = J_f = 2A/(d_{Co} + d_{Cu})$ where in the layer under study the thickness of the Co layer was $d_{Co} = 2$ nm and of the Cu layer $d_{Cu} = 1$ nm [7].

All results presented below were obtained for a multilayer containing six magnetic layers. Each layer was discretized in $N_x \times N_z = 65 \times 65$ cells with physical cell sizes $\Delta x = \Delta z = 2$ nm. The defect geometry is shown in Fig. 1. Defect region occupied two discretization cells in the x-direction and 48 cells in the z-direction.

During micromagnetic simulations we applied free boundary conditions to the upper and lower magnetic layers, fixed boundary conditions for the left and right cell layers (magnetization orientation which would be obtained for a perfect multilayer, as in Ref. [6]; it can be calculated using, i.e., the so-called 'atomic layer model', see Ref. [7] for the latest example of such calculations) and 'infinity' boundary conditions to the front and back cell layers. 'Infinity' boundary conditions mean that by the exchange energy evaluation (the only energy contribution which depends on the boundary condition) we assumed that moment orientations in the cell layer before the front layer are exactly the same as in the front layer and in the layer behind the back layer – the same as in the back layer. This assumptions mean that front and back layers are supposed to be so far (hence the 'infinity' boundary conditions) from the defect end that practically no magnetization changes occur along the y-axis (see Fig. 1) outside the simulated region.

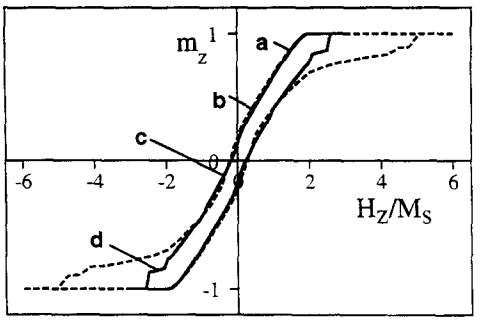

Fig. 2. Hysteresis loops for the multilayer structures with the semi-infinite defect shown in Fig. 1 (solid line) and with the structure with the same parameters but the infinite defect (dashed line). Points on the hysteresis loop which were used to generate Lorentz microscopy images shown in Figs. 5 and 6 are marked as a, b, c and d.

To simulate a hysteresis loop we started from a large external field ($H_0 \geqslant 10M_s$) where the system was almost saturated and computed the equilibrium magnetization state using the equation-of-motion algorithm [9]. Then we decreased the field a little bit and used the equilibrium structure obtained in the previous field as a starting one for the new equilibration process. Hysteresis loops obtained this way are shown in Fig. 2 (see next section for details).

3. Numerical simulation results and Lorentz microscopy observations of 360° domain walls

The basic difference between hysteresis loops obtained for the semi-infinite defect shown in Fig. 1 and for the infinite defect with the same depth and width but infinitely long in z-direction (shown in Fig. 2 with the solid and dashed lines correspondingly) is the large reduction of the annihilation field of 360°-domain walls for the semi-infinite defect. This reduction manifests itself in the decrease of the field where the hysteresis loop closes – the so-called irreversibility field H_{irr} [5]. In addition, for the semi-infinite defect this irreversibility field was found to depend strongly on the defect configuration, i.e., on the number of layers occupied by the defect region, on the defect width in the x-direction (see Fig. 1), etc. Corresponding dependencies for the infinite defect are much weaker.

This indicates that the magnetization configuration near the defect end plays a very important role in the formation and annihilation of 360°-domain walls. To visualize these processes, we show the configuration of magnetic moments around the defect end for a layer where a 360°-domain wall is formed (Fig. 3); we would like to recall that for

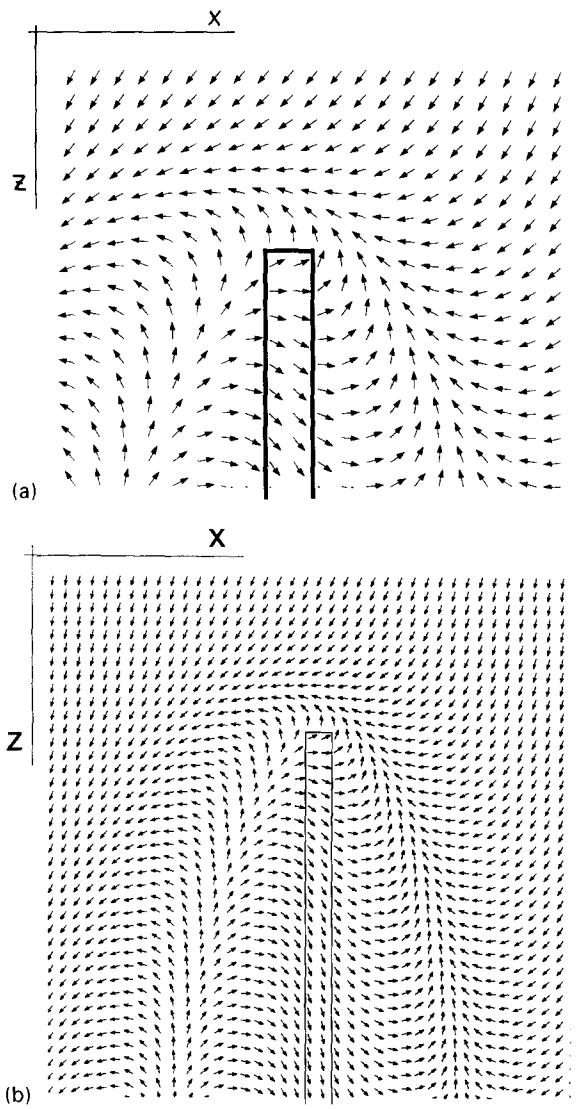

Fig. 3. (a) Curled magnetization structure near the end of defect in a magnetic layer where 360°-domain wall is formed. (b) A pair of 360°-domain walls formed around the semi-infinite linear defect. Both pictures corresponds to the state marked as d on the hysteresis loop in Fig. 2.

defect shape studied here such walls are formed in each second layer containing a defect as explained in detail in Ref. [6], p. 3.1. It can be seen that a pair of such walls is formed around the defect region (shown with the solid rectangle) and that these walls are 'pinned' at the end of defect. This 'pinning' occurs due to the formation of the curl-like magnetization structure near the defect end (Fig. 3a). The reason for formation of this curl is the same as for the 360°-domain wall itself: moments far from the defect region are coupled to the adjacent magnetic layers antiferromagnetically, whereas moments in the defect region are coupled ferromagnetically, so that during the remagnetization process they are forced to rotate with opposite rotation senses.

Far away from the defect line the energetically most favorable position for both walls is in the middle between this line and the borders of the simulated structure which are held fixed by the boundary conditions. This follows from the symmetry reasons at least in a strong negative field where moments near the defect and on the borders of the simulated structure are saturated in the negative z-direction. Hence, starting near the defect end both walls tend to 'move away' from the defect line when the distance to the defect end increases thus forming a Λ-like structure (Fig. 3b).

To verify the formation mechanism of 360° domain walls proposed here we have performed Lorentz microscopy observations of the remagnetization process in our multilayer structures. Multilayers with 12 Co layers (each 2 nm thick) separated by 1 nm Cu spacer layers were used. Lorentz microscopy images during the remagnetization were recorded using the technique described in Ref. [10] (similar images recorded during the remagnetization of the biased Permalloy layer can be found in Ref. [11]). A typical picture obtained this way is shown in Fig. 4. Black and white lines oriented nearly perpendicular to the field direction can be clearly recognized. As explained in Ref. [10] these lines correspond to 360° walls with opposite magnetization rotation senses. The inset in Fig. 4 shows the enlarged image of the Λ-like structure corresponding to those presented in Fig. 3b and Fig. 5d. The walls also were found to appear approximately on the same places during repeated remagnetization cycles, as it would be the case if

Fig. 4. Lorentz microscopy picture observed during the remagnetization process for our multilayers (see text for layer parameters) in the field $H_x = 90$ Oe. Note that the black–white structures corresponding to 360° domain walls lie approximately perpendicular to the field direction.

they formation would be determined by the structural defects.

However, drastic quantitative discrepancies between experimental observations and simulation results were found. First of all, the field region for which such walls could be observed was much narrower than found in our simulation (approximately one order of magnitude). But, as it is already mentioned above, this field region strongly depends on the defect parameters serving as input for our micromagnetic model so that this discrepancy can be easily removed.

More serious is the disagreement of numerical results concerning the wall width ($l_{\text{sim}} \approx 20$ nm, see Fig. 3 and Ref. [6]) with the wall width determined experimentally. The latter (measured using the method described in Ref. [10]) was found to be $l_{\text{exp}} \approx 150 \pm 10$ nm (the averaging was performed over ~ 200 values). As it was pointed out in Ref. [5] the wall width observed in simulated structures does not depend on the defect parameters at all, but depends only on the magnetic and structural properties of a perfect multilayer.

Indeed, for the mechanism of the wall formation proposed in Ref. [6] such a wall appears as a consequence of opposite rotation directions of the magnetization in some layer within the defect region and far away from it (due to the AF coupling to adjacent layers outside the defect region and FM coupling near the defect). The width of a wall formed this way can be estimated exactly as that of a usual 180°-degree walls in uniaxial materials ($l_w \sim \sqrt{A/K}$). The role of the uniaxial anisotropy constant K in our situation plays the combination of AF interlayer coupling constant J_{af} and magnetic layer thickness d_{Co}: $K_{\text{eff}} = |J_{\text{af}}|/d_{\text{Co}}$, so that the wall thickness in our multilayer should be $l_w \sim 2\sqrt{Ad_{\text{Co}}/|J_{\text{af}}|}$ (a factor 2 arises due to 360° wall instead of usual 180°-wall in uniaxial materials).

Substituting into the above estimate for the wall width structural and magnetic parameters of our multilayer (for concrete values of A, d_{Co} and J_{af} see text after Eq. (1)) we obtain a wall width $l_w \sim 20$ nm which is in a very good agreement with the numerically simulated magnetization pattern. The drastic disagreement of this value with the experimentally determined wall width $l_w \sim 150$ nm leads to the conclusion that 360° walls found on the Lorentz microscopy images were formed via another mechanism than that proposed by us in Refs. [5, 6]. The observation that domain walls detected experimentally lie approximately perpendicular to the applied field (see Fig. 4) is another hint that a different mechanism is responsible for the formation of these walls. If the wall formation would be governed only by the directions of defect lines then the directions of corresponding domain walls would be random due to random orientations of linear defects. We suggest that the formation of the ripple-like structures in our multilayers could also be responsible for the initial stage of 360° domain wall formation. Further studies of this question are under way.

To complete our comparison with the experimental data, we have also performed numerical simulations of the Lorentz microscopy images which would be obtained during the remagnetization process from the multilayer regions near the end of the defects where structures like those shown in Fig. 3 could be formed. The Lorentz images were calculated in a usual way, i.e., we assumed that (i) a sample was irradiated with an electron beam with a homogeneous intensity and the propagation direction perpendicular to the layer plane and (ii) after passing the layer the Lorentz deviation

angle of the beam behind the given sample point is proportional to the net magnetization across the layer at this point. The deviation angle per unit magnetization and the distance between the layer plane and the plane where the beam intensity was registered were chosen to ensure the maximal contrast of the pictures presented below.

In such a model both in the saturated state (the magnetization is homogeneous and hence the electron beam is deviated uniformly) and in the remanence state for a perfect AF coupled multilayer (no external field, the net magnetization is zero, no deviation of the electron beam at all) a uniformly grey image would be observed. For a multilayer

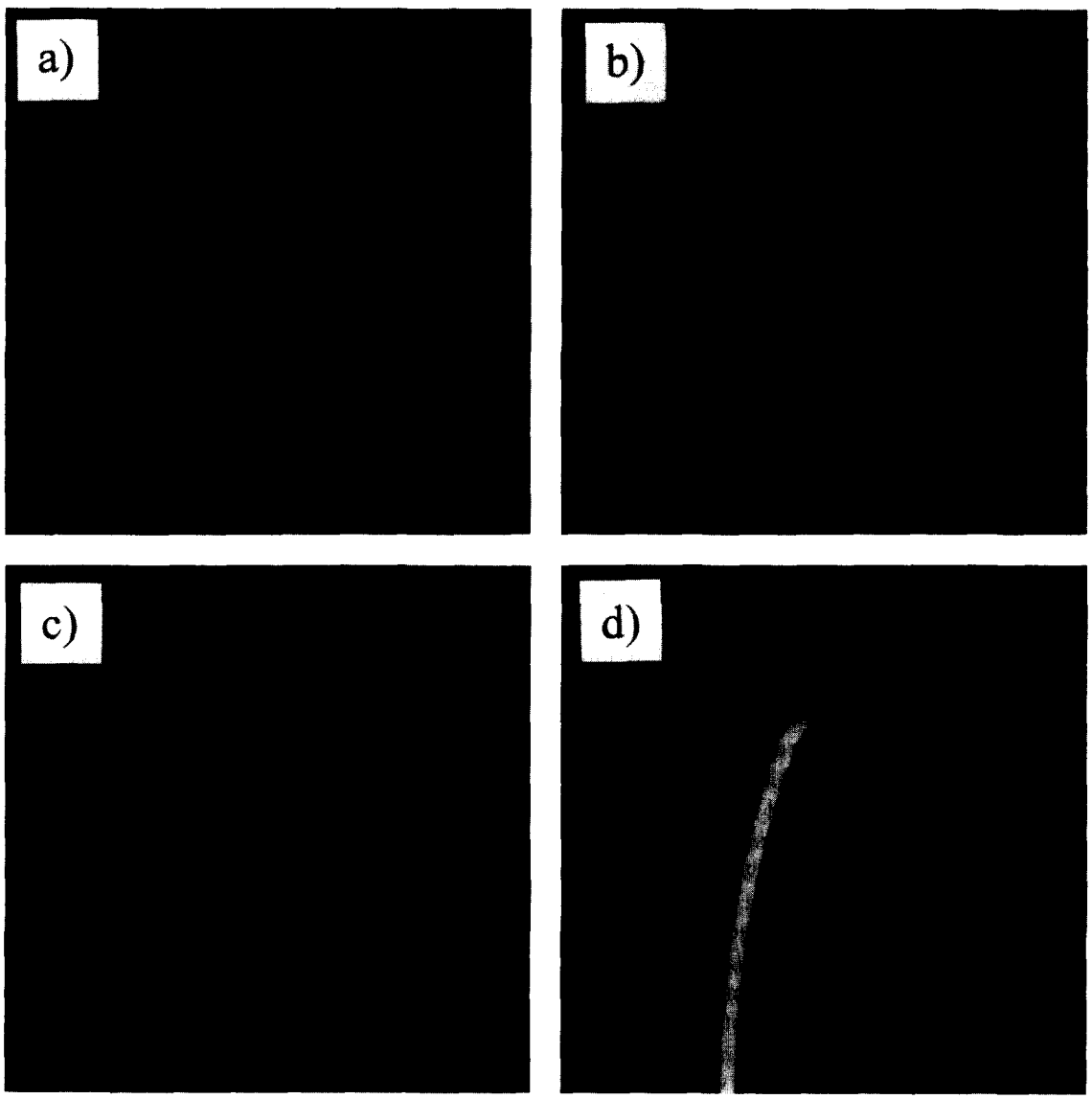

Fig. 5. Simulated Lorentz microscopy images of a magnetization structure occurring in a defect multilayer for various magnetic fields. Corresponding points are marked on the hysteresis loop in Fig. 2 with the same letters as parts of this figure. External field is directed perpendicular to the defect line.

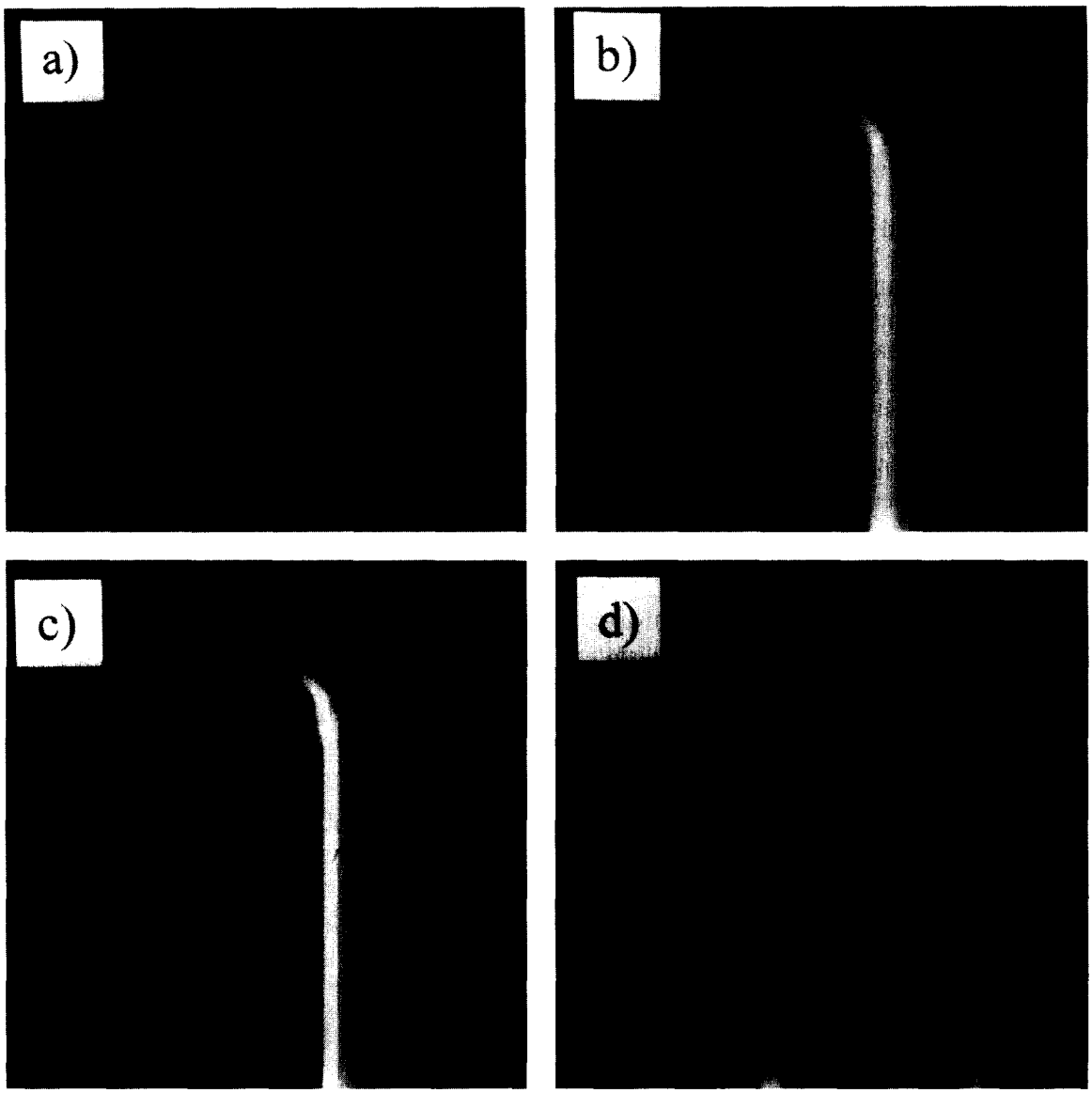

Fig. 6. The same as in Fig. 5 for the field direction parallel to the defect line.

containing a defect the inhomogeneous magnetization structure occurring around this defect during the remagnetization lead to complicate Lorentz images shown for various stages of this process in Figs. 5 and 6 for the external field lying in the layer plane perpendicular (Fig. 5) and parallel (Fig. 6) to the defect line. Note, that pictures obtained for 360° domain walls lying approximately perpendicular to the field direction (Fig. 6d) are in a qualitative agreement with images observed experimentally (Fig. 4): (i) pairs of thick black–white lines which would result from the pair of 360° domain walls

accompaining each defect and (ii) Λ-like structures formed by these pairs which would occur near the end of defects can be clearly seen.

4. Summary

We have extended the 2D model of a straight infinitely long linear defect in AF coupled multilayers to 3D which allowed us to study the case of a finite defect. The main differences to the previous model are the formation of Λ-like domain wall structures due to the pinning of domain walls near the end of the defect and large reduction of the annihilation field for such walls. The magnitude of this annihilation field strongly depends on the magnetic and geometric defect parameters. However, the wall width obtained in our model does not depend on these parameters and is much less than that observed experimentally. This leads to the conclusion that even if structural defects are responsible for the appearance of such walls, the equilibrium parameters (width, magnetization configuration, energy) are governed by another mechanisms.

Acknowledgements

The authors greatly acknowledge valuable discussions with Prof. W. Andrä.

References

[1] R. Mattheis, W. Andrä, L. Fritzsch, J. Langer, S. Schmidt, J. Appl. Phys. 76 (1994) 6510.
[2] G. Rupp, H.A.M. van den Berg, IEEE Trans. Magn. 29 (1993) 3102.
[3] H.A.M. van den Berg, S. Schmeusser, IEEE Trans. Magn. 29 (1993) 3099.
[4] U. Gradmann, H.J. Elmers, J. Magn. Magn. Mater. 137 (1994) 44.
[5] R. Mattheis, W. Andrä, D. Berkov, J. Magn. Magn. Mater. 154 (1996) 24.
[6] D.V. Berkov, N.L. Gorn, W. Andrä, R. Mattheis, S. Schmidt, Phys. Stat. Sol. (a) 158 (1996) 247.
[7] W. Andrä, H.A.M. van den Berg, H. Danan, R. Mattheis, G. Rupp, S. Schmidt, J. Magn. Magn. Mater. 148 (1995) 223.
[8] C. Kittel, Rev. Mod. Phys. 21 (1949) 541.
[9] D.V. Berkov, K. Ramstöck, A. Hubert, Phys. Stat. Sol. (a) 137 (1993) 207.
[10] T. Zimmermann, Ph.D. Thesis, Universität Regensburg, 1996.
[11] M.F. Gillies, J.N. Chapman, J.C.S. Kools, J. Appl. Phys. 78 (1995) 5554.